



Antagonistic Effects of Ocean Acidification and Rising Sea Surface Temperature on the Dissolution of Coral Reef Carbonate Sediments

Daniel Trnovsky^{1*}, Laura Stoltenberg¹, Tyler Cyronak² and Bradley D. Eyre¹

¹ Centre for Coastal Biogeochemistry, School of Environment, Science and Engineering, Southern Cross University, Lismore, NSW, Australia, ² Scripps Institution of Oceanography, University of California, San Diego, La Jolla, CA, USA

OPEN ACCESS

Edited by:

Hajime Kayanne,
University of Tokyo, Japan

Reviewed by:

Juan Pablo Carricart-Ganivet,
National Autonomous University of
Mexico, Mexico
Lyndon Mark DeVantier,
Coral Reef Research and Museum of
Tropical Queensland, Australia

*Correspondence:

Daniel Trnovsky
d.trnovsky.10@student.scu.edu.au

Specialty section:

This article was submitted to
Coral Reef Research,
a section of the journal
Frontiers in Marine Science

Received: 29 July 2016

Accepted: 12 October 2016

Published: 02 November 2016

Citation:

Trnovsky D, Stoltenberg L, Cyronak T
and Eyre BD (2016) Antagonistic
Effects of Ocean Acidification and
Rising Sea Surface Temperature on
the Dissolution of Coral Reef
Carbonate Sediments.
Front. Mar. Sci. 3:211.
doi: 10.3389/fmars.2016.00211

Increasing atmospheric CO₂ is raising sea surface temperature (SST) and increasing seawater CO₂ concentrations, resulting in a lower oceanic pH (ocean acidification; OA), which is expected to reduce the accretion of coral reef ecosystems. Although sediments comprise most of the calcium carbonate (CaCO₃) within coral reefs, no *in situ* studies have looked at the combined effects of increased SST and OA on the dissolution of coral reef CaCO₃ sediments. *In situ* benthic chamber incubations were used to measure dissolution rates in permeable CaCO₃ sands under future OA and SST scenarios in a coral reef lagoon on Australia's Great Barrier Reef (Heron Island). End of century (2100) simulations (temperature +2.7°C and pH -0.3) shifted carbonate sediments from net precipitating to net dissolving. Warming increased the rate of benthic respiration (R) by 29% per 1°C and lowered the ratio of productivity to respiration (P/R; ΔP/R = -0.23), which increased the rate of CaCO₃ sediment dissolution (average net increase of 18.9 mmol CaCO₃ m⁻² d⁻¹ for business as usual scenarios). This is most likely due to the influence of warming on benthic P/R which, in turn, was an important control on sediment dissolution through the respiratory production of CO₂. The effect of increasing CO₂ on CaCO₃ sediment dissolution (average net increase of 6.5 mmol CaCO₃ m⁻² d⁻¹ for business as usual scenarios) was significantly less than the effect of warming. However, the combined effect of increasing both SST and pCO₂ on CaCO₃ sediment dissolution was non-additive (average net increase of 5.6 mmol CaCO₃ m⁻² d⁻¹) due to the different responses of the benthic community. This study highlights that benthic biogeochemical processes, such as metabolism and associated CaCO₃ sediment dissolution respond rapidly to changes in SST and OA, and that the response to multiple environmental changes are not necessarily additive.

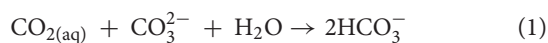
Keywords: sediment, calcium carbonate, dissolution, ocean acidification, sea surface temperature

INTRODUCTION

Human induced disruptions to the global carbon cycle are having profound environmental effects across Earth's continents and oceans (Pachauri et al., 2014). Carbon dioxide (CO₂) concentrations are increasing in both the atmosphere and oceans, primarily due to the burning of fossil fuels and deforestation. This has driven an increase in the global mean sea surface temperature (SST)

of $\sim 0.7^{\circ}\text{C}$ since pre-industrial times (Hoegh-Guldberg et al., 2007) and depending on future emissions scenarios, average SST is predicted to increase by a further 1.2 to 3.2°C by the end of this century (Gattuso et al., 2015). The oceans have also absorbed almost one third of anthropogenically produced CO_2 (Sabine et al., 2004), which has had considerable effects on seawater carbonate chemistry, lowering seawater pH in a process termed ocean acidification (OA) (Doney et al., 2009). To date, there has been a ~ 0.1 reduction in surface seawater pH compared to the pre-industrial era (Orr et al., 2005; Feely et al., 2009), and a further reduction of up to 0.3 units by the end of the century is predicted under a “business as usual” carbon emission scenario (Gattuso et al., 2015).

Increasing seawater CO_2 concentration also drives changes in the seawater carbonate system that lowers the concentration of carbonate (CO_3^{2-}) ions according to Equation 1.



A reduction in CO_3^{2-} concentration lowers the calcium carbonate saturation state (Ω) of a specific calcium carbonate mineral (CaCO_3) phase (Morse and Mackenzie, 1990). The calcium carbonate saturation state is a measure of the thermodynamic potential for CaCO_3 to precipitate or dissolve in seawater, where net precipitation is favored in seawater with a $\Omega > 1$ and net dissolution in seawater with a $\Omega < 1$ (Zeebe and Wolf-Gladrow, 2001). Decreasing pH and Ω are likely to have a negative impact on the production, accumulation and dissolution of CaCO_3 minerals within coral reefs and other oceanic environments (Hoegh-Guldberg et al., 2007; Eyre et al., 2014; Cyronak et al., 2016).

The persistence and accretion of coral reef ecosystems is dependent on positive rates of net ecosystem calcification (NEC; gross calcification minus gross CaCO_3 dissolution occurring within the reef; Andersson and Gledhill, 2013). The reduction in seawater pH and Ω due to OA is expected to decrease rates of calcification (Gattuso et al., 1999; Langdon et al., 2000) and increase rates of CaCO_3 dissolution (Andersson et al., 2009; Cyronak et al., 2013a), which will both negatively affect NEC. Most dissolution probably occurs within the pore waters of coral reef sediments which comprise the majority of CaCO_3 in reef ecosystems (Eyre et al., 2014). The dominant mineral phase of CaCO_3 in shallow coral reef sediments are aragonite and high magnesium calcite (Morse and Arvidson, 2002), and reefs are generally confined to waters with aragonite saturation states (Ω_{Ar}) > 1 . However, sediment pore waters can become under saturated with respect to Ω_{Ar} due to the remineralization of organic matter and other sedimentary processes (Ku et al., 1999; Andersson and Gledhill, 2013; Andersson, 2015). Ocean acidification can increase the rate of sediment dissolution as low Ω_{Ar} surface seawater is advected into the pore waters (Cyronak et al., 2013a). Because permeable carbonate sediments make up a large percentage of the benthic areal coverage of coral reef ecosystems, their increased dissolution rates under OA scenarios could play a significant role in future changes to coral reef NEC (Eyre et al., 2014; Cyronak and Eyre, 2016).

While there is increasing evidence that OA increases the dissolution rates of exposed reef structure and sediments (Andersson et al., 2007; Cyronak et al., 2013a; Comeau et al., 2015; Cyronak and Eyre, 2016), and that SST is a major environmental control on the rate of coral growth (Lough and Cooper, 2011) little is known about the combined effects of increasing SST and OA. Increasing SST will increase Ω_{Ar} which influences the dissolution and precipitation of CaCO_3 minerals. However, within the range of the temperature increase expected over the coming century, the effect on Ω_{Ar} will be small (~ 0.026 increase in Ω_{Ar} per 1°C increase; Pierrot et al., 2006). Increased SST may also result in increased metabolic activity of benthic organisms, such as benthic microalgae (BMA) and bacteria (Hancke and Glud, 2004). Rising SST has been shown to increase rates of calcification on reefs, most likely due to a combination of enhanced coral metabolism and increased photosynthetic rates of symbiotic algae (Lough and Barnes, 2000; McNeil et al., 2004). However, little is known about the effect of rising SST on CaCO_3 dissolution in coral reef sediments.

Benthic respiration (R) and productivity (P) alter the concentration of dissolved inorganic carbon (DIC) in the sediment pore water with R releasing CO_2 into the pore waters and photosynthesis consuming CO_2 . In laboratory studies increasing SST generally exerts a stronger influence on R than P, shifting aquatic ecosystems toward heterotrophy (Hancke and Glud, 2004; Yvon-Durocher et al., 2010; Tait and Schiel, 2013; Hancke et al., 2014). This has also been shown *in situ* by studies that examined the relationship between SST and metabolism under seasonal changes in temperature (Kristensen, 1993; Yap et al., 1994). Any increase in the ratio of production to respiration (P/R) would increase pore water Ω_{Ar} through the uptake of CO_2 and a decrease in P/R would have the opposite effect. Therefore, changes to the balance of P/R due to increasing temperature in coral reef sediments may have an important effect on CaCO_3 dissolution (Cyronak and Eyre, 2016).

To our knowledge no *in situ*, manipulative studies have examined the relationship between temperature, sediment metabolism and CaCO_3 dissolution. We hypothesize that increasing SST and CO_2 will individually increase the rate of sediment dissolution and that the combined effect will be additive. To test this hypothesis, we conducted replicated, *in situ* advective benthic chamber incubations with manipulations of CO_2 and SST, individually and in combination, in sediments at Heron Island, Australia.

METHODS AND MATERIALS

Study Site

This study was carried out at Heron Island in Australia's Great Barrier Reef Marine Park. Heron Island is a densely wooded, 8 ha sand cay situated on the Tropic of Capricorn. The island is bordered by a shallow coral reef flat and lagoon composed mostly of coarse CaCO_3 sands interspersed with coral clusters (Glud et al., 2008). The carbonate sands, which cover 85% of the reef flat and lagoon are highly permeable, filtering $\sim 15\%$ of the lagoon volume each day (Wild et al., 2004). The study site, a sandy patch on the reef flat, was located about 100 m from

shore to the south-west of the island. The sediment at the study site is composed almost entirely of CaCO_3 sediment dominated by aragonite (65%) and high magnesium calcite (34%) (Cyronak et al., 2013b).

Experimental Design

This study investigated changes in CaCO_3 dissolution under simulated future ocean CO_2 and temperature scenarios. The IPCC has described four different emissions scenarios (Representative Concentration Pathways; RCPs) likely to occur during the twenty first century. The changes in seawater pH and temperature were designed to reflect predicted values under the RCP 4.5 (intermediate; $\Delta\text{SST} + 1.28^\circ\text{C}$ and $\Delta\text{pH} -0.15$) and RCP 8.5 (“business as usual;” $\Delta\text{SST} + 2.73^\circ\text{C}$ and $\Delta\text{pH} -0.33$) (Gattuso et al., 2015). Rates of CaCO_3 dissolution and precipitation, as well as organic respiration and photosynthesis, were measured in nine advective benthic chambers. Three sets of nine chamber incubations were carried out for 24 h at the same site. Each set of chamber incubations consisted of a control and two treatments, performed in triplicate. To measure the effect of increasing SST on dissolution rates, temperature of the treatments was raised by ~ 1.3 and 2.7°C above ambient, offset from the natural diel variability in temperature (Figure 1A). To measure the effect of increasing $p\text{CO}_2$ on carbonate sediment dissolution rates CO_2 was added until the pH of the overlying water was reduced by ~ 0.2 and 0.4 units (Figure 1E). To measure the combined effect of temperature and CO_2 we conducted two treatments; an intermediate treatment where temperature was increased by 1.3°C in combination with a 0.2 unit decrease in pH, and a business as usual treatment consisting of a 2.7°C increase in temperature in combination with a 0.4 unit decrease in pH (Figures 1C,F).

Benthic Chambers

Advective benthic chambers, with a height of 330 mm and an internal diameter of 190 mm, were fitted with a stirring disc 50 mm below the top of the chamber. The disc was set to stir at 40 revolutions per minute which induces an advection rate of $\sim 43 \text{ L m}^{-2} \text{ d}^{-1}$ in the sediments at the study site (Glud et al., 2008). The base of each chamber was inserted into the sediment, away from any visible macro-fauna or burrows, to a depth of 100–120 mm, enclosing a water column 190–230 mm above the sediment. The height of the chambers above the sediment was measured and used to calculate the volume of water held within each chamber. The chamber lids were fitted after the chambers were allowed to sit for ~ 1 h while any disturbed sediment settled. One Onset HOBO pendant temperature/light data logger was attached to the inside of each chamber lid and set to log temperature every 5 min. Temperature, pH, dissolved oxygen (DO) and salinity of the water column was recorded every 30 min by a SeapHOx sensor (Bresnahan et al., 2014) deployed beside the chambers.

Temperature and CO_2 Manipulations

The first set of incubations was a temperature manipulation (T) at ambient $p\text{CO}_2$ which ran from dusk on October 12 to dusk on October 13, 2015. The incubation consisted of three control

chambers, three treatment chambers set to $1.3 \pm 0.4^\circ\text{C}$ (Mid-T) and three treatment chambers set to $2.7 \pm 0.5^\circ\text{C}$ (High-T) above controls. Temperature manipulations in the chambers were accomplished using small 12V silicone heating pads (Jiangying Mengyou, China) suspended halfway between the sediment and the top of the chamber. To achieve the desired offset in SST, 5 W heaters were used in the Mid-T treatments and 10 W heaters were used in the High-T treatments. The heaters were installed and started ~ 1.5 h prior to dusk (i.e., the first sampling point) to allow a temperature offset to be established. The temperature offset was maintained on top of the natural diel temperature cycle in the chambers (Figures 1A,D).

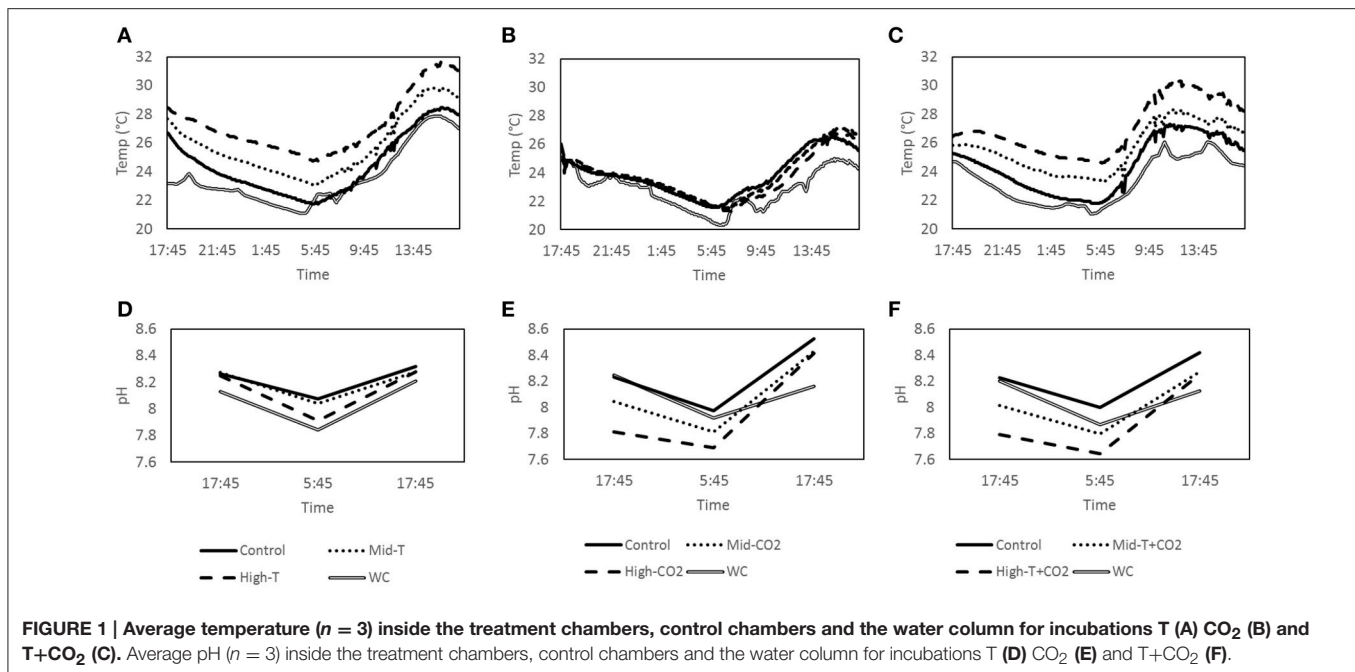
The second set of incubations was a $p\text{CO}_2$ manipulation (CO_2) run at ambient temperature. It ran from dusk on October 16 to dusk on October 17 2015. Similarly, the incubation consisted of three control chambers, three chambers at a pH offset of -0.20 ± 0.02 (Mid- CO_2) and three at a pH offset of -0.42 ± 0.02 (High- CO_2). A 1 L bottle of seawater was saturated with CO_2 by bubbling pure CO_2 through the water until it stabilized at $\text{pH} \sim 5.0$. This low pH seawater was injected into the chambers via a syringe in order to establish an offset in overlying seawater pH (30 ml into the Mid- CO_2 treatments and 50 ml into the High- CO_2 treatments). pH was measured 5 min after the initial addition and further small additions of low pH seawater were added where necessary to reach the nominated pH offset for each treatment. The pH offset was maintained on top of the natural diel pH cycle in the chambers (Figures 1B,E) as shown in previous studies (Cyronak et al., 2013a).

The third set of incubations was a combined temperature and $p\text{CO}_2$ manipulation (T+ CO_2). It ran from dusk on October 20 to dusk on October 21 2015. Three control chambers were left at ambient temperature and $p\text{CO}_2$. Three treatment chambers were heated to $+1.2 \pm 0.2^\circ\text{C}$ and acidified with CO_2 enriched water to achieve a pH offset of -0.19 ± 0.02 (Mid-T+ CO_2). The final three chambers were heated to $+2.6 \pm 0.1^\circ\text{C}$ and acidified with CO_2 enriched seawater to a pH offset of -0.43 ± 0.01 (High-T+ CO_2). Unfortunately, one of the High-T+ CO_2 chambers was lost during the experiment resulting in only two replicates. The temperature and pH offsets were maintained on top of the natural diel cycles in temperature and pH within the chambers (Figures 1C,F).

Sample Collection and Analysis

Seawater samples (120 ml total) were taken from the chambers via two 60 ml syringes at dusk, dawn and the following dusk for all incubations. The samples were brought back to the laboratory for immediate analysis and preservation. Unfiltered samples were analyzed for DO (mg L^{-1}), using a Hach HQ 30d Flexi meter and Luminescent Dissolved Oxygen (LDO[®]) probe. Samples for total alkalinity (TA) were $0.45 \mu\text{m}$ filtered to remove fine particulate carbonate and kept in 40 ml plastic, airtight containers with no headspace and analyzed within 12 h. Unfiltered DIC samples were poisoned using a saturated solution of mercuric chloride, stored in 20 ml glass, airtight containers and analyzed within 10 days.

Total Alkalinity (TA) was determined by Gran titrations using a Metrohm 888 Titrando automatic titrator. Dickson



certified reference material (Batch 144) was used to calibrate pre-standardized hydrochloric acid and to estimate error ($\text{SD} = \pm 4.1 \mu\text{mol kg}^{-1}$). Duplicates of samples were analyzed approximately every three samples and the averages of each data point were used. The average standard deviation of duplicate samples was $\pm 4.4 \mu\text{mol kg}^{-1}$ ($n = 30$). DIC was measured using a Marianda AIRICA and Li-COR LI 7000 $\text{CO}_2/\text{H}_2\text{O}$ Analyzer. Four measurements were taken for each sample with the poorest (greatest deviation from the mean) rejected and the concentration ($\mu\text{mol L}^{-1}$) calculated from the average of the remaining three. The average standard error of all measurements was $\pm 0.54 \mu\text{mol L}^{-1}$. Ω_{Ar} and pH were calculated using the Excel macro CO_2SYS (Pierrot et al., 2006) with constants set to Mehrbach et al. (1973) refit by Dickson and Millero (1987). DIC and TA measurements were used as inputs for the carbonate chemistry parameters, salinity inputs were taken from the SeapHOx measurements and temperature from the HOBO data loggers for the appropriate chamber and time point. All HOBO temperatures were corrected to the Sea-Bird temperature logger in the SeapHOx.

Temperature Correction

The HOBO temperature data were cross-calibrated among the nine units and against the Sea-Bird temperature logger in the SeapHOx. A single HOBO unit was placed alongside the SeapHOx and set to log every 5 min for 24 h. The two temperature loggers tracked closely overnight but as the sun rose and the water temperature increased the HOBO logged consistently read higher temperatures than the SeapHOx, which may reflect heating inside the transparent plastic HOBO casing (Bahr et al., 2016). A correction factor was calculated for every half hour of daylight and applied to the recorded HOBO

temperature. This correction was applied to all data obtained from HOBO data loggers during the experiment.

Calculation of Fluxes

TA measurements were converted from $\mu\text{mol kg}^{-1}$ into $\mu\text{mol L}^{-1}$ using density calculated from the salinity and temperature of the water at the time of measurement. Fluxes of DO, TA, and DIC were calculated as follows;

$$F = \frac{\Delta S \times V}{A \times \Delta T} \quad (2)$$

where ΔS is the change in solute concentration in $\mu\text{mol L}^{-1}$, V is the volume in L of water within the chamber, A is the area in m^2 of sediment covered by the chamber and ΔT is the time elapsed between measurements in hours. F is the rate of solute flux in $\mu\text{mol m}^{-2} \text{h}^{-1}$. Positive values of F represent solute fluxes from the sediment into the water column while negative values indicate solute fluxes from the water column into the sediment.

Rates of net CaCO_3 dissolution/precipitation were inferred from TA fluxes using the alkalinity anomaly technique (Kinsey, 1978; Chisholm and Gattuso, 1991). TA fluxes were multiplied by 0.5 as two moles of alkalinity are produced/consumed for every one mole of CaCO_3 dissolved/precipitated. It is assumed that all TA produced or consumed within the chambers was due to calcium carbonate dissolution or precipitation, which has been validated in previous studies using Ca^{2+} fluxes (Rao et al., 2012). TA fluxes, converted to CaCO_3 dissolution and precipitation are termed dissolution (D) where positive values represent net dissolution and negative values represent net precipitation. Fluxes were calculated during the daytime (D_{LIGHT}), night time (D_{DARK}) and over the full 24-h incubation (D_{NET}). Fluxes of DIC were corrected for changes in DIC due to

CaCO₃ precipitation/dissolution by subtracting the dissolution flux from the DIC flux (DIC_{TA}). Because respiration consumes one mole of O₂ for every mole of CO₂ produced (CH₂O + O₂ → H₂O + CO₂), the DO flux from the sediment should roughly equal the DIC_{TA} flux if there are no other sources of alkalinity (e.g., sulfate reduction). DO fluxes were also used to calculate rates of respiration ($R = \text{dark DO flux} \times -1$), net primary production ($\text{NPP} = \text{light DO flux}$), gross primary production ($\text{GPP} = \text{NPP} + R$), and the ratio of production to respiration ($\text{P/R} = \text{GPP} \times 12 \text{ (daylight hs)}/R \times 24$) (Eyre et al., 2011). Q₁₀ values were calculated to determine the factor by which both GPP and R increase when the temperature is raised by 10° using the following equation.

$$Q_{10} = \left(\frac{M_2}{M_1} \right)^{\left(\frac{10}{T_2 - T_1} \right)} \quad (3)$$

M₁ is the metabolic rate (GPP or R) at temperature T₁ and M₂ is the rate of P or R at temperature T₂, where T₁ < T₂.

To remove any inter-day variability due to naturally changing conditions, such as light, Δ from control fluxes were calculated allowing for comparisons between incubations that were carried out on separate days. Fluxes in the control chambers were averaged ($n = 3$) and subtracted from the fluxes in each treatment chamber. Students *t*-tests and analyses of variance (ANOVA) were performed using Microsoft Excel, with reported *p*-values referring to *t*-tests unless otherwise mentioned. Levene's tests were used test for homogeneity of variance and regression analysis was performed using Microsoft Excel. Results are expressed as mean ± standard error of the mean (SE), unless mentioned otherwise.

RESULTS

Temperature Effects

Water temperature in the control chambers for all three sets of incubations followed a diel cycle driven by changes in sunlight and tides. This diel cycle was similar to the water column but the average temperature in control chambers over the three experiments was between 0.7 and 1.1°C warmer than the water column (Table 1). However, temperature offsets in the treatments during these incubations tracked the diel fluctuations closely. Mean temperature offsets were +1.3 ± 0.4°C (Mid-T) and +2.7 ± 0.5°C (High-T) in the two treatments (Figure 1A, Table 1).

Increasing temperature had an influence on organic metabolism, with R ($p < 0.002$; Figure 2A), GPP ($p < 0.002$; Figure 2B), and P/R ($p = 0.028$; Figure 2C) significantly correlated to temperature. In all incubations involving temperature manipulations, increasing SST increased the rate of both R (Figure 3A) and GPP (Figure 3B). In the temperature only incubations, increasing T increased R by 29% per 1°C and Q₁₀ values ranged from 7.4 to 13.0 for R and from 3.1 to 4.1 for GPP. P/R was lower in both Mid-T and High-T incubations (Figure 4B), with no significant difference between the two treatments ($p = 0.72$). The pooled average of ΔP/R in both the Mid-T and High-T treatments ($n = 6$) was significantly lower than controls ($\Delta\text{P/R} = -0.24 \pm 0.06$; $p =$

0.024; Figure 4D). The decrease in P/R with increasing average temperature indicates that R was preferentially stimulated over P by increasing SST.

Increasing temperature also had an important effect on CaCO₃ dissolution/precipitation. D_{DARK} was significantly correlated with R ($r^2 = 0.67$, $p < 0.002$; Figures 2D, 4B,E), while D_{LIGHT} showed no correlation with GPP ($p = 0.96$; Figures 2E, 4C,F). P/R was negatively correlated to D_{NET} on a daily basis, however, the correlation was not significant ($P = 0.06$; Figure 2F). Control chambers during the temperature incubation were net CaCO₃ precipitating over the diel cycle ($D_{\text{NET}} = -6.9 \pm 4.4 \text{ mmol CaCO}_3 \text{ m}^{-2} \text{ d}^{-1}$) while Mid-T chambers were approximately balanced and not significantly different from controls ($D_{\text{NET}} = -0.6 \pm 1.5 \text{ mmol CaCO}_3 \text{ m}^{-2} \text{ d}^{-1}$; $p = 0.15$). The High-T treatment was net dissolving and significantly different from the controls ($D_{\text{NET}} = 12.0 \pm 1.0 \text{ mmol CaCO}_3 \text{ m}^{-2} \text{ d}^{-1}$; $p = 0.026$). The average difference in ΔD_{NET} between controls and treatments was +6.2 ± 1.5 and +18.9 ± 1.0 mmol CaCO₃ m⁻² d⁻¹ for the Mid-T and High-T treatments, respectively (Figure 4A).

CO₂ Effects

In the CO₂ incubation pH within the chambers followed diel cycles similar to that in the water column (Figure 1E). The offsets diminished slightly throughout the incubation but pH remained significantly lower than controls until the end of the incubations ($p = 0.02$). The average pH offsets were -0.15 ± 0.03 and -0.28 ± 0.01 for Mid-CO₂ and High-CO₂, respectively (Table 1).

The addition of CO₂ at ambient temperature increased P/R compared to the controls in both treatments, however, there was no significant difference between Mid-CO₂ and High-CO₂ ($p = 0.15$) treatments. The pooled average of the two treatments ($n = 6$) was significantly higher than controls ($\Delta\text{P/R} = 0.15 \pm 0.07$; $p = 0.04$; Figure 4D). The CO₂ treatments had average D_{NET} rates higher than controls but there was no significant difference between controls and the two treatments (ANOVA $p = 0.33$; Levene's test $p = 0.79$). The difference in D_{NET} between controls and the CO₂ treatments was 2.3 ± 3.3 mmol CaCO₃ m⁻² d⁻¹ (Mid-CO₂) and 6.5 ± 2.7 mmol CaCO₃ m⁻² d⁻¹ (High-CO₂) (Figure 4A). D_{DARK} rates, however, did increase significantly in both Mid-CO₂ (0.68 ± 0.30 mmol CaCO₃ m⁻² h⁻¹; $p = 0.032$) and High-CO₂ (1.09 ± 0.30 mmol CaCO₃ m⁻² h⁻¹; $p = 0.006$) treatments (Figure 4B).

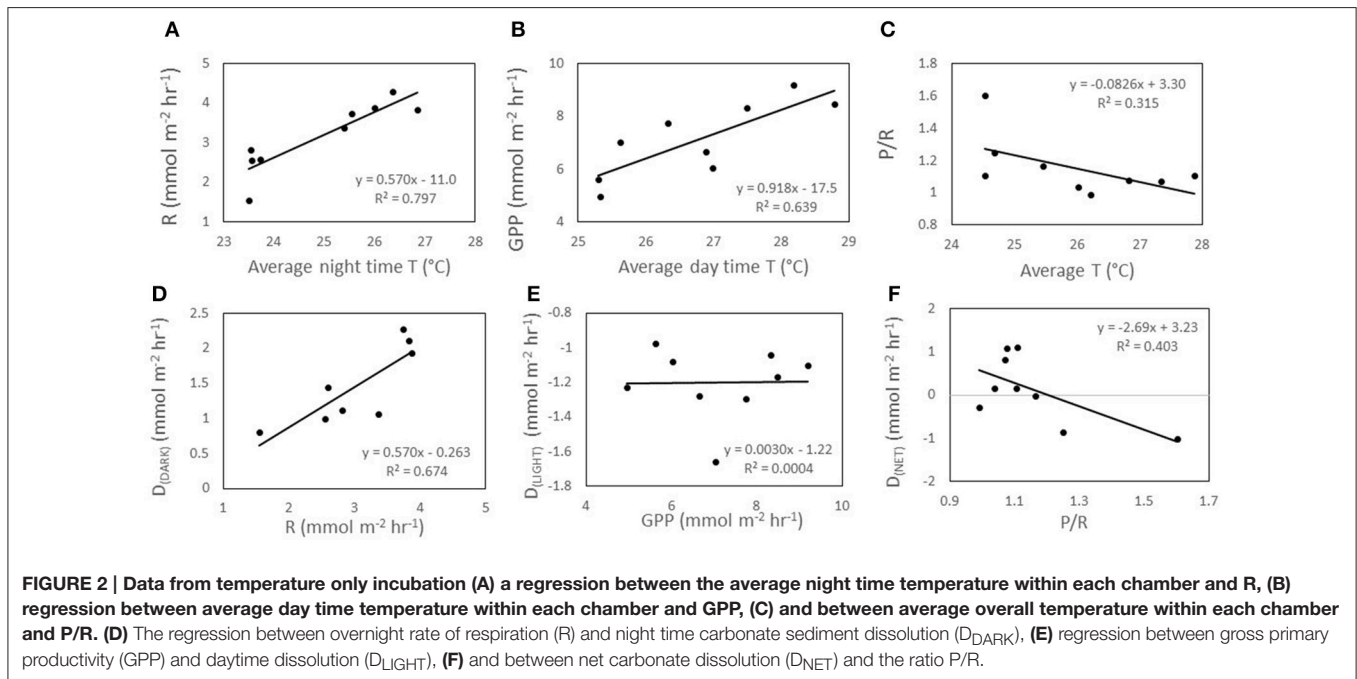
Combined Effects of Temperature and CO₂

Average pH offsets in the T+CO₂ incubation were -0.19 (±0.02) and -0.33 (±0.01) for Mid-T+CO₂ and High-T+CO₂, respectively (Table 1). pH offsets diminished slightly throughout the incubation but remained significantly lower than controls until the end of the incubations ($p = 0.004$). Temperature offsets were +1.2 ± 0.2°C (Mid-T+CO₂) and +2.6 ± 0.1°C (High-T+CO₂) (Figure 1F, Table 1).

The difference in D_{NET} between controls and Mid-T+CO₂ ($n = 3$) was 5.5 ± 1.7 mmol CaCO₃ m⁻² d⁻¹ and 5.7 ± 3.0 mmol CaCO₃ m⁻² d⁻¹ for High-T+CO₂ ($n = 2$; Figure 4A). ΔD_{NET} in the Mid treatments was not significantly different across the three

TABLE 1 | Shows average \pm SD ($n = 3$; except High-T+CO₂ $n = 2$) values for pH, Ω_{Ar} , and temperature in controls and treatments for each incubation and the water column.

	T			CO ₂			T+CO ₂		
	pH	Ω_{Ar}	Temp (°C)	pH	Ω_{Ar}	Temp (°C)	pH	Ω_{Ar}	Temp (°C)
Control	8.18 \pm 0.05	3.77 \pm 0.15	24.51 \pm 0.05	8.18 \pm 0.02	3.74 \pm 0.15	23.85	8.16 \pm 0.04	3.41 \pm 0.30	24.41 \pm 0.06
Mid	8.16 \pm 0.05	3.83 \pm 0.12	25.85 \pm 0.23	8.03 \pm 0.04	2.99 \pm 0.25	23.67	7.97 \pm 0.06	2.41 \pm 0.17	25.61 \pm 0.15
High	8.09 \pm 0.02	3.72 \pm 0.06	27.31 \pm 0.31	7.90 \pm 0.04	2.53 \pm 0.07	23.91	7.83 \pm 0.03	2.74 \pm 0.68	27.05 \pm 0.03
Water column	8.04 \pm 0.11		23.80 \pm 1.96	8.06 \pm 0.09		22.77 \pm 1.14	8.07 \pm 0.09		23.63 \pm 1.64



incubations (ANOVA $p = 0.48$), however, there was a significant difference between high CO₂ treatments and controls (ANOVA $p = 0.02$). ΔD_{NET} was significantly greater in the High-T than in the High-T+CO₂ treatments ($p = 0.01$). Average ΔD_{NET} was not significantly different between Mid-T and Mid-CO₂ ($p = 0.16$), however, average ΔD_{NET} for High-T was significantly greater than for High-CO₂ ($p = 0.007$).

P/R decreased in the Mid-T+CO₂ and High-T+CO₂ treatments compared to controls (Figure 4A; $\Delta P/R = -0.13 \pm 0.08$), however, the difference between controls and the two treatments was not significant (ANOVA $p = 0.30$; Levene's test $p = 0.50$). The temperature increase at ambient CO₂ had a greater effect on P/R than at increased CO₂ (Figure 4A). Q_{10} values for the T+CO₂ incubation ranged from 1.1 to 2.1 for R and 0.4 and 1.6 for GPP.

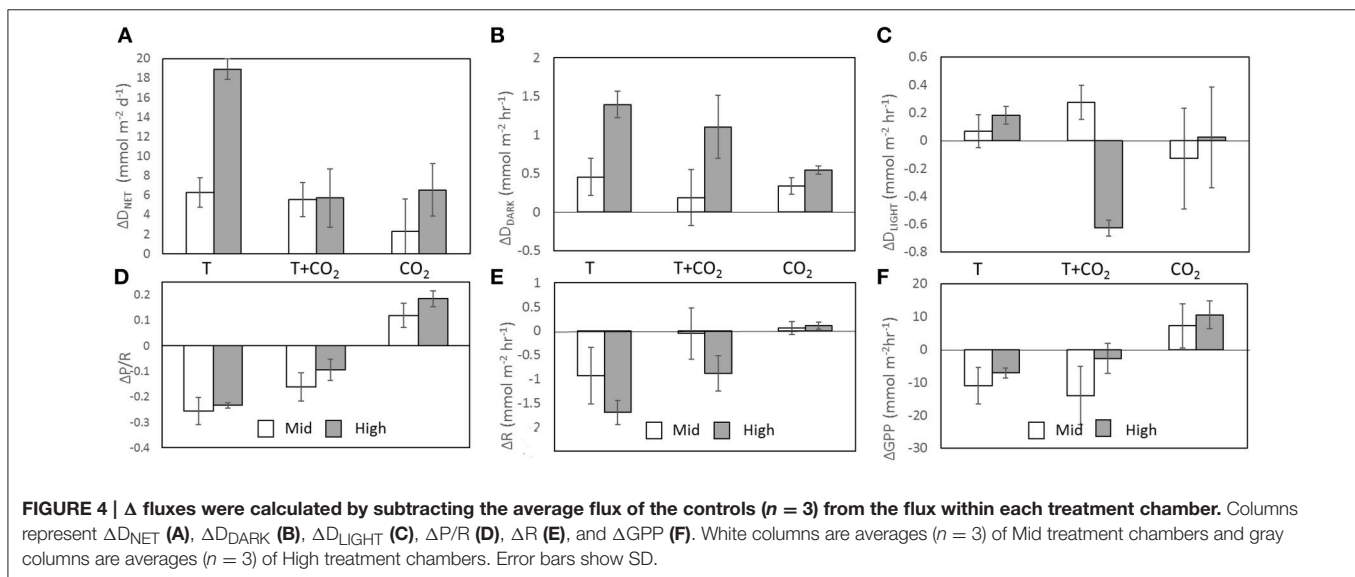
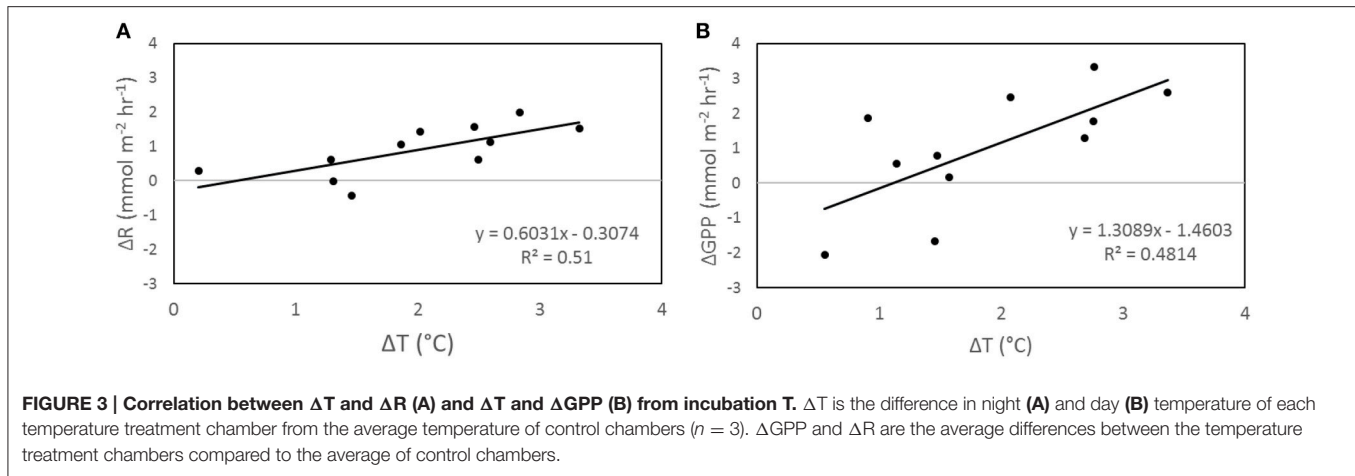
The greatest increase in D_{NET} from controls to treatments was observed in the temperature only incubation which also showed the greatest decrease in P/R. In the CO₂ incubation, $\Delta P/R$ was positive and ΔD_{NET} was the smallest of the three incubations. Both ΔD_{NET} and $\Delta P/R$ for the T+CO₂ incubation were in between the two individual stressor treatments (Figure 5).

DISCUSSION

Effect of Warming on Benthic Metabolism and Sediment Dissolution

Warming significantly increased both GPP and R, while the net balance of P/R was lowered (Figures 2, 3). Q_{10} for R in the temperature only incubation was high (7.4–13.0) when typically, Q_{10} values for biological systems are no greater than 2.5 (Valiela, 1995; Davidson et al., 2006). However, Q_{10} has been shown to vary based on the temperatures that it is calculated at with higher Q_{10} values at lower temperatures (Schipper et al., 2014). The lower Q_{10} for GPP compared to R explains the change in P/R driven by warming. The changes in P/R led to an overall increase in sediment dissolution (Figures 4A,D). Figure 5 demonstrates how temperature exerts an influence on P/R by lowering it, which in turn influences the rate of D_{NET} , increasing it. This is most likely due to increased R increasing pore water CO₂ and the rate of metabolic dissolution within the sediments (Eyre et al., 2014; Cyronak and Eyre, 2016).

Provided benthic microalgae (BMA) are adapted to an optimal temperature higher than that of the present SST, and no other factors are limiting growth, warming should result in increased



metabolic activity (Beardall and Raven, 2004) which is theorized to have a greater effect on R than P (López-Urrutia et al., 2006). For example, modeling by Allen et al. (2005) investigating plant, animal and microbial metabolism predicts a 3.8-fold increase in the rate of photosynthesis over the temperature range 0–30°C compared to a 16-fold increase for R. Manipulative studies looking at the effect of temperature on GPP and R also show a greater influence of warming on R, making aquatic systems more heterotrophic. For example, this has been shown in BMA in temperate and high-arctic subtidal sediments (Hancke and Glud, 2004; Hancke et al., 2014), in macro-algal assemblages in southern New Zealand (Tait and Schiel, 2013) and in a freshwater lake ecosystem in the United Kingdom (Yvon-Durocher et al., 2010). Our results show that the same preferential increase in R over P will occur in BMA in tropical coral reef sediments.

Similarly, there have been a number of field studies showing how seasonal temperature changes exert a greater effect on R than GPP in BMA (Kristensen, 1993; Yap et al., 1994; Smith and Kemp, 1995). For example, a study of both R and GPP in

coral reef sediments over the course of 2 years found a positive relationship between temperature and R but no significant relationship between temperature and GPP (Yap et al., 1994). In a shallow oligotrophic, marine lagoon in Denmark, seasonal changes in temperature exerted a greater control on R ($r^2 = 0.83–0.87$) than GPP ($r^2 = 0.67–0.72$) (Kristensen, 1993). Two stations nearest the ocean in Chesapeake Bay, USA shifted from net autotrophy in the winter to near zero net metabolism in summer, when SST increased (Smith and Kemp, 1995). These field studies support the changes in net metabolism observed in our chambers under increasing SST, and warrant further studies investigating changing sediment metabolism under natural seasonal cycles in SST at Heron Island.

The changes in benthic metabolism associated with warming increased net carbonate sediment dissolution by 6.2 ± 1.5 mmol $m^{-2} d^{-1}$ in the Mid-T and 18.9 ± 1.0 mmol $CaCO_3 m^{-2} d^{-1}$ in the High-T treatments. Increased benthic metabolism, in the temperature range of this experiment, overshadowed any geochemical effect (i.e., increases in Ω_{Ar} due to increasing

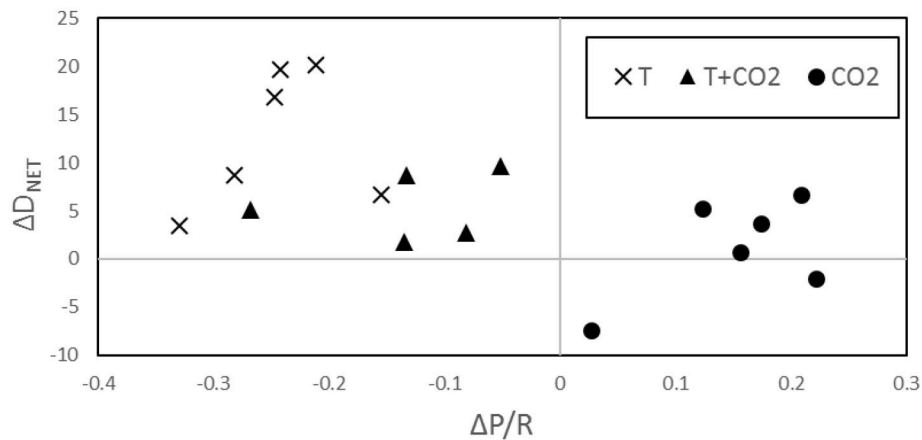


FIGURE 5 | Plot of ΔD_{NET} vs. $\Delta P/R$ for each incubation.

temperature). This is because the increases in temperature considered in this experiment would have only a small thermodynamic impact on Ω_{Ar} (Morse and Mackenzie, 1990). However, the strong effect of temperature on organic metabolism played a critical role in regulating CaCO_3 dissolution, which is similar to another study that manipulated GPP through light limitation (Cyronak and Eyre, 2016). Algal photosynthesis and respiration have been found to increase with temperature up to a point, and then decline rapidly (Davison, 1991). Therefore, the response of CaCO_3 dissolution to increasing SST observed here cannot be predicted to increase linearly beyond the temperature range investigated.

Effect of Elevated CO_2 on Benthic Metabolism and Sediment Dissolution

The addition of CO_2 at ambient temperature had no significant effect on NPP (ANOVA $p = 0.53$), GPP (ANOVA $p = 0.65$) or R (ANOVA $p = 0.83$). P/R, on average, increased in both treatments compared to controls ($+0.15 \pm 0.07$; $n = 6$), and $\Delta P/R$ was significantly greater than zero (One-sample t-test; $p = 0.003$). Elevated $p\text{CO}_2$ increased D_{DARK} rates significantly by $0.68 \pm 0.30 \text{ mmol CaCO}_3 \text{ m}^{-2} \text{ h}^{-1}$ ($p = 0.032$) and $1.09 \pm 0.30 \text{ mmol CaCO}_3 \text{ m}^{-2} \text{ h}^{-1}$ ($p = 0.006$) for average Ω_{Ar} changes of -0.75 and -1.21 , respectively. However, D_{NET} was not significantly different from controls in either the Mid- or High CO_2 treatments. This result is not consistent with a number of other studies investigating the effects of $p\text{CO}_2$ on carbonate sediment dissolution, and may be due to the increases of P/R in both CO_2 treatments (Figure 5). For example, in a previous *in situ* study at the same site, Cyronak et al. (2013a) found that an average Ω_{Ar} offset of -1.1 led to an average increase in net carbonate sediment dissolution over controls of $0.49 (\pm 0.19) \text{ mmol CaCO}_3 \text{ m}^{-2} \text{ h}^{-1}$. Comeau et al. (2014), used flumes to study the effect of increased $p\text{CO}_2$ on the dissolution and precipitation of coral reef sediments from Moorea. Similarly, they reported an increase in net sediment dissolution ($\sim 0.75 \text{ mmol CaCO}_3 \text{ m}^{-2} \text{ h}^{-1}$) under high $p\text{CO}_2$

($\sim 900 \mu\text{atm}$). Andersson et al. (2007) studied carbonate sediment dissolution under conditions of elevated $p\text{CO}_2$ (up to $2000 \mu\text{atm}$) where thermally driven density stratification in Devil's Hole, Bermuda, produced $p\text{CO}_2$ levels similar to or higher than those levels anticipated by the end of the twenty first century ($\sim 700 \mu\text{atm}$). Likewise, they report that carbonate sediments are subject to increased dissolution (0.3 to $1.6 \text{ mmol CaCO}_3 \text{ m}^{-2} \text{ h}^{-1}$) under conditions of elevated $p\text{CO}_2$.

Combined Effect of Warming and Increased CO_2 on Benthic Metabolism and Sediment Dissolution

During the temperature only incubations R and GPP were positively correlated to increasing temperature ($r^2 = 0.80$, $p < 0.002$, and 0.64 , $p < 0.002$ for R and GPP, respectively; Figures 2A,B). In contrast, during the combined temperature and CO_2 incubations these relationships were much weaker and not significant ($r^2 = 0.25$, $p = 0.20$, and $r^2 = 0.12$, $p = 0.40$ for R and GPP, respectively). This is potentially due to increases in P/R driven by higher CO_2 concentrations. Furthermore, Q_{10} values for both R and GPP were much lower in the T+ CO_2 incubation compared to the T incubation. The presence of excess CO_2 appeared to temper the effect of temperature on benthic metabolism. The metabolism of benthic organisms will most likely change in different ways for different species as a response to stress (Gibson et al., 2012), and it is possible that excess CO_2 was causing additional stresses, such as hypercapnia (Fabry et al., 2008) or fueling more production by the BMA.

This contrasting response of the benthic community to warming and CO_2 enrichment is consistent with a number of other studies. Reynaud et al. (2003) found that warming increased photosynthesis in a scleractinian coral but that the effect diminished when CO_2 was increased. Sorte and Bracken (2015) found that algal NPP increased in response to increased temperature in tidal pools in Alaska but not when warming was combined with increased CO_2 . In mesocosm experiments

Olabarria et al. (2013) also found that NPP of macro algae was typically higher in warmed treatments and that this effect was less pronounced when CO₂ was also increased. Sorte and Bracken attribute the increase in algal NPP under warming to favorable changes in C:N, which are potentially negated by reduced C affinity, lower HCO₃⁻ utilization, reduced Rubisco content, and decreased pigment concentrations under increased pCO₂.

Rather than having an additive effect, as we expected, the combined effect of warming and increased pCO₂ on net carbonate sediment dissolution was less than that of warming alone. Combined, warming and elevated pCO₂ increased average net carbonate sediment dissolution by 5.5 ± 1.7 mmol CaCO₃ m⁻² d⁻¹ and 5.7 ± 3.0 mmol CaCO₃ m⁻² d⁻¹ in the Mid-T+CO₂ and High-T+CO₂ treatments, respectively. The decrease in P/R driven by warming (Figure 2C) was depressed when combined with increased CO₂ (Figure 5), which would have resulted in relatively increased Ω_{Ar} and lower dissolution rates.

Potential Artifacts of the Experiment

While *in situ* temperature and pCO₂ manipulation experiments clearly have many advantages over controlled laboratory and mesocosm studies, they are not without potential issues. Only short-term experiments (24 h) were undertaken to avoid containment effects within the benthic chambers. However, the benthic community may acclimatize over longer timescales, and temper the response to temperature and pCO₂ changes. Furthermore, average temperature and pH in the control chambers were slightly higher than that of the water column, mostly due to the chamber trapping warmer, higher pH water at the end of the day when the chambers were closed. This could result in metabolic rates within the chambers that are artificially higher than under natural conditions outside of the chambers. However, because all of the chambers were started at the same time and experienced similar starting conditions this doesn't preclude comparison between treatments

Secondly, the incubations were carried out at the end of spring when average SST was not at its highest. Mean monthly SST on Heron Island reef flat varies by as much as 8°C from winter to summer (AIMS, 2015). Therefore, warming may have had a different effect on dissolution if the experiments were run in winter or summer. If summer ambient temperatures were closer to the upper temperature limit of the BMA, then increasing SST may inhibit metabolism rather than enhance it. Alternatively, in

winter when starting temperatures are below the optimum for benthic metabolism, the effect of increased SST may be even more pronounced.

Finally, this study has again highlighted the importance of P/R in controlling sediment biogeochemical processes (e.g., Ferguson et al., 2004; Eyre et al., 2008, 2011), including dissolution (Cyronak and Eyre, 2016). However, it was undertaken in shallow water and P/R is expected to vary greatly across different water depths. Studies that incorporate multiple diel cycles and seasons at different locations and depths are required to determine the longer-term effect of rising SST on benthic metabolism, pCO₂ and CaCO₃ dissolution.

CONCLUSIONS

We predicted that increasing pCO₂ would increase the rate of sediment dissolution and that, while increasing SST may increase Ω values, buffering this effect, the biological effect of SST on benthic metabolism, pCO₂ and dissolution would be stronger than the geochemical effect. We found that increases in SST increased the rate of benthic respiration relative to photosynthesis, in turn, increasing pCO₂, lowering Ω and increasing the rate of dissolution in carbonate sediments. Despite the fact that the combined effects of increased pCO₂ and SST were not additive it is unlikely that increasing SST will help buffer the effect of OA on the dissolution of CaCO₃ sediments and NEC. In fact, changes to metabolism driven by increasing SST may compound any effects of OA. To fully understand how temperature will affect carbonate dissolution in an acidifying ocean further studies should look at the longer-term effects of temperature and its interaction with increased pCO₂ on the metabolism of benthic organisms.

AUTHOR CONTRIBUTIONS

DT and BE conceived the project, BE and TC supervised and advised the methods, DT and LS performed the experiments, DT analyzed the data and wrote the paper with contributions from all authors.

ACKNOWLEDGMENTS

This project was funded by ARC Discovery Grant DP150102092.

REFERENCES

- AIMS (2015). *Water Temperature at Heron Island Reef Flat [Online]*. Australian Institute of Marine Science AIMS web publications. Available online at: <http://data.aims.gov.au/aimsrtds/datatool.xhtml?Qc=level2&channels=1838> (Accessed February 11, 2016).
- Allen, A., Gillooly, J., and Brown, J. (2005). Linking the global carbon cycle to individual metabolism. *Funct. Ecol.* 19, 202–213. doi: 10.1111/j.1365-2435.2005.00952.x
- Andersson, A. J. (2015). A fundamental paradigm for coral reef carbonate sediment dissolution. *Front. Mar. Sci.* 2:52. doi: 10.3389/fmars.2015.00052
- Andersson, A. J., Bates, N. R., and Mackenzie, F. T. (2007). Dissolution of carbonate sediments under rising pCO₂ and ocean acidification: observations from Devil's Hole, Bermuda. *Aquatic Geochem.* 13, 237–264. doi: 10.1007/s10498-007-9018-8
- Andersson, A. J., and Gledhill, D. (2013). Ocean acidification and coral reefs: effects on breakdown, dissolution, and net ecosystem calcification. *Ann. Rev. Mar. Sci.* 5, 321–348. doi: 10.1146/annurev-marine-121211-172241
- Andersson, A., Kuffner, I., Mackenzie, F., Jokiel, P., Rodgers, K., and Tan, A. (2009). Net loss of CaCO₃ from a subtropical calcifying community due to seawater acidification: mesocosm-scale experimental evidence. *Biogeosciences* 6, 1811–1823. doi: 10.5194/bg-6-1811-2009
- Bahr, K. D., Jokiel, P. L., and Rodgers, K. U. S. (2016). Influence of solar irradiance on underwater temperature recorded by temperature loggers on coral reefs. *Limnol. Oceanogr. Methods* 14, 338–342. doi: 10.1002/lom3.10093

- Beardall, J., and Raven, J. A. (2004). The potential effects of global climate change on microalgal photosynthesis, growth and ecology. *Phycologia* 43, 26–40. doi: 10.2216/i0031-8884-43-1-26.1
- Bresnahan, P. J., Martz, T. R., Takeshita, Y., Johnson, K. S., and Lashomb, M. (2014). Best practices for autonomous measurement of seawater pH with the Honeywell Durafet. *Methods Oceanogr.* 9, 44–60. doi: 10.1016/j.mio.2014.08.003
- Chisholm, J. R., and Gattuso, J. P. (1991). Validation of the alkalinity anomaly technique for investigating calcification of photosynthesis in coral reef communities. *Limnol. Oceanogr.* 36, 1232–1239. doi: 10.4319/lo.1991.36.6.1232
- Comeau, S., Carpenter, R. C., Lantz, C. A., and Edmunds, P. J. (2015). Ocean acidification accelerates dissolution of experimental coral reef communities. *Biogeosciences* 12, 365–372. doi: 10.5194/bg-12-365-2015
- Comeau, S., Edmunds, P. J., Lantz, C. A., and Carpenter, R. C. (2014). Water flow modulates the response of coral reef communities to ocean acidification. *Sci. Rep.* 4:6681. doi: 10.1038/srep06681
- Cyronak, T., and Eyre, B. D. (2016). The synergistic effects of ocean acidification and organic metabolism on calcium carbonate (CaCO₃) dissolution in coral reef sediments. *Mar. Chem.* 183, 1–12. doi: 10.1016/j.marchem.2016.05.001
- Cyronak, T., Santos, I. R., and Eyre, B. D. (2013a). Permeable coral reef sediment dissolution driven by elevated pCO₂ and pore water advection. *Geophys. Res. Lett.* 40, 4876–4881. doi: 10.1002/grl.50948
- Cyronak, T., Santos, I. R., McMahon, A., and Eyre, B. D. (2013b). Carbon cycling hysteresis in permeable carbonate sands over a diel cycle: implications for ocean acidification. *Limnol. Oceanogr.* 58, 131–143. doi: 10.4319/lo.2013.58.1.0131
- Cyronak, T., Schulz, K. G., and Jokiel, P. L. (2016). The Omega myth: what really drives lower calcification rates in an acidifying ocean. *ICES J. Mar. Sci.* 73, 558–562. doi: 10.1093/icesjms/fsv075
- Davidson, E. A., Janssens, I. A., and Luo, Y. (2006). On the variability of respiration in terrestrial ecosystems: moving beyond Q10. *Glob. Change Biol.* 12, 154–164. doi: 10.1111/j.1365-2486.2005.01065.x
- Davison, I. R. (1991). Environmental effects on algal photosynthesis: temperature. *J. Phycol.* 27, 2–8. doi: 10.1111/j.0022-3646.1991.00002.x
- Dickson, A., and Millero, F. (1987). A comparison of the equilibrium constants for the dissociation of carbonic acid in seawater media. *Deep Sea Res. A. Oceanogr. Res. Pap.* 34, 1733–1743. doi: 10.1016/0198-0149(87)90021-5
- Doney, S. C., Fabry, V. J., Feely, R. A., and Kleypas, J. A. (2009). Ocean acidification: the other CO₂ problem. *Mar. Sci.* 1, 169–192. doi: 10.1146/annurev.marine.010908.163834
- Eyre, B. D., Andersson, A. J., and Cyronak, T. (2014). Benthic coral reef calcium carbonate dissolution in an acidifying ocean. *Nat. Climate Change* 4, 969–976. doi: 10.1038/nclimate2380
- Eyre, B. D., Ferguson, A. J., Webb, A., Maher, D., and Oakes, J. M. (2011). Metabolism of different benthic habitats and their contribution to the carbon budget of a shallow oligotrophic sub-tropical coastal system (southern Moreton Bay, Australia). *Biogeochemistry* 102, 87–110. doi: 10.1007/s10533-010-9424-7
- Eyre, B. D., Glud, R. N., and Patten, N. (2008). Mass coral spawning: a natural large-scale nutrient addition experiment. *Limnol. Oceanogr.* 53:997. doi: 10.4319/lo.2008.53.3.0997
- Fabry, V. J., Seibel, B. A., Feely, R. A., and Orr, J. C. (2008). Impacts of ocean acidification on marine fauna and ecosystem processes. *ICES J. Mar. Sci.* 65, 414–432. doi: 10.1093/icesjms/fsn048
- Feely, R. A., Doney, S. C., and Cooley, S. R. (2009). Ocean acidification: present conditions and future changes in a high-CO₂ world. *Oceanography* 22, 36–47. doi: 10.5670/oceanog.2009.95
- Ferguson, A. J. P., Eyre, B. D., and Gay, J. (2004). Benthic nutrient fluxes in euphotic sediments along shallow sub-tropical estuaries, northern NSW, Australia. *Aquatic Microb. Ecol.* 37, 219–235. doi: 10.3354/ame037219
- Gattuso, J.-P., Allemand, D., and Frankignoulle, M. (1999). Photosynthesis and calcification at cellular, organismal and community levels in coral reefs: a review on interactions and control by carbonate chemistry. *Am. Zool.* 39, 160–183. doi: 10.1093/icb/39.1.160
- Gattuso, J.-P., Magnan, A., Billé, R., Cheung, W. W. L., Howes, E. L., Joos, F., et al. (2015). Contrasting futures for ocean and society from different anthropogenic CO₂ emissions scenarios. *Science* 349:aac4722. doi: 10.1126/science.aac4722
- Gibson, R., Atkinson, R., Gordon, J., Hughes, R., Hughes, D., and Smith, I. (2012). Benthic invertebrates in a high-CO₂ world. *Oceanogr. Mar. Biol.* 50, 127–188.
- Glud, R. N., Eyre, B. D., and Patten, N. (2008). Biogeochemical responses to mass coral spawning at the Great Barrier Reef: effects on respiration and primary production. *Limnol. Oceanogr.* 53, 1014–1024. doi: 10.4319/lo.2008.53.3.1014
- Hancke, K., and Glud, R. N. (2004). Temperature effects on respiration and photosynthesis in three diatom-dominated benthic communities. *Aquatic Microb. Ecol.* 37, 265–281. doi: 10.3354/ame037265
- Hancke, K., Sorell, B. K., Lund-Hansen, L. C., Larsen, M., Hancke, T., and Glud, R. N. (2014). Effects of temperature and irradiance on a benthic microalgal community: a combined two-dimensional oxygen and fluorescence imaging approach. *Limnol. Oceanogr.* 59, 1599–1611. doi: 10.4319/lo.2014.59.5.1599
- Hoegh-Guldberg, O., Mumby, P. J., Hooten, A. J., Steneck, R. S., Greenfield, P., Gomez, E., et al. (2007). Coral reefs under rapid climate change and ocean acidification. *Science* 318, 1737–1742. doi: 10.1126/science.1152509
- Kinsey, D. W. (1978). Alkalinity changes and coral reef calcification. *Limnol. Oceanogr.* 23, 989–991. doi: 10.4319/lo.1978.23.5.0989
- Kristensen, E. (1993). Seasonal variations in benthic community metabolism and nitrogen dynamics in a shallow, organic-poor Danish lagoon. *Estuar. Coast. Shelf Sci.* 36, 565–586. doi: 10.1006/ecss.1993.1035
- Ku, T. C. W., Walter, L. M., Coleman, M. L., Blake, R. E., and Martini, A. M. (1999). Coupling between sulfur recycling and syndepositional carbonate dissolution: evidence from oxygen and sulfur isotope composition of pore water sulfate, South Florida Platform, U.S.A. *Geochim. Cosmochim. Acta* 63, 2529–2546. doi: 10.1016/S0016-7037(99)00115-5
- Langdon, C., Takahashi, T., Sweeney, C., Chipman, D., Goddard, J., Marubini, F., et al. (2000). Effect of calcium carbonate saturation state on the calcification rate of an experimental coral reef. *Global Biogeochem. Cycles*, 14, 639–654. doi: 10.1029/1999GB001195
- López-Urrutia, Á., San Martín, E., Harris, R. P., and Irigoien, X. (2006). Scaling the metabolic balance of the oceans. *Proc. Natl. Acad. Sci.* 103, 8739–8744. doi: 10.1073/pnas.0601137103
- Lough, J. M., and Barnes, D. J. (2000). Environmental controls on growth of the massive coral Porites. *J. Exp. Mar. Biol. Ecol.* 245, 225–243. doi: 10.1016/S0022-0981(99)00168-9
- Lough, J., and Cooper, T. (2011). New insights from coral growth band studies in an era of rapid environmental change. *Earth Sci. Rev.* 108, 170–184. doi: 10.1016/j.earscirev.2011.07.001
- McNeil, B. I., Matear, R. J., and Barnes, D. J. (2004). Coral reef calcification and climate change: the effect of ocean warming. *Geophys. Res. Lett.* 31:L22309. doi: 10.1029/2004gl021541
- Mehrbach, C., Culberson, C., Hawley, J., and Pytkowicz, R. (1973). Measurement of the apparent dissociation constants of carbonic acid in seawater at atmospheric pressure. *Limnol. Oceanogr.* 18, 897–907. doi: 10.4319/lo.1973.18.6.0897
- Morse, J. W., and Arvidson, R. S. (2002). The dissolution kinetics of major sedimentary carbonate minerals. *Earth Sci. Rev.* 58, 51–84. doi: 10.1016/S0012-8252(01)00083-6
- Morse, J. W., and Mackenzie, F. T. (1990). *Geochemistry of Sedimentary Carbonates*. Burlington, NC: Elsevier.
- Olabarria, C., Arenas, F., Viejo, R. M., Gestoso, I., Vaz-Pinto, F., Incera, M., et al. (2013). Response of macroalgal assemblages from rockpools to climate change: effects of persistent increase in temperature and CO₂. *Oikos* 122, 1065–1079. doi: 10.1111/j.1600-0706.2012.20825.x
- Orr, J. C., Fabry, V. J., Aumont, O., Bopp, L., Doney, S. C., Feely, R. A., et al. (2005). Anthropogenic ocean acidification over the twenty-first century and its impact on calcifying organisms. *Nature* 437, 681–686. doi: 10.1038/nature04095
- Pachauri, R. K., Allen, M., Barros, V., Broome, J., Cramer, W., Christ, R., et al. (2014). *Climate Change 2014. Synthesis Report, Contribution of Working Groups I, II and III to the Fifth Assessment Report of the Intergovernmental Panel on Climate Change*.
- Pierrot, D., Lewis, D. E., and Wallace, D. W. R. (2006). *MS Excel Program Developed for CO₂ System Calculations*. Oak Ridge, TN: Carbon Dioxide Information Analysis Center; Oak Ridge National Laboratory; US Department of Energy.
- Rao, A. M. F., Polerecky, L., Ionescu, D., Meysman, F. J. R., and de-Beer, D. (2012). The influence of pore-water advection, benthic photosynthesis, and respiration on calcium carbonate dynamics in reef sands. *Limnol. Oceanogr.* 57, 809–825. doi: 10.4319/lo.2012.57.3.0809
- Reynaud, S., Leclercq, N., Romaine-Lioud, S., Ferrier-Pagés, C., Jaubert, J., and Gattuso, J. P. (2003). Interacting effects of CO₂ partial pressure

- and temperature on photosynthesis and calcification in a scleractinian coral. *Glob. Chang Biol.* 9, 1660–1668. doi: 10.1046/j.1365-2486.2003.00678.x
- Sabine, C. L., Feely, R. A., Gruber, N., Key, R. M., Lee, K., Bullister, J. L., et al. (2004). The oceanic sink for anthropogenic CO₂. *Science* 305, 367–371. doi: 10.1126/science.1097403
- Schipper, L. A., Joanne, K. H., Rutledge, S., and Arcus, V. L. (2014). Thermodynamic theory explains the temperature optima of soil microbial processes and high Q₁₀ values at low temperatures. *Glob. Chang Biol.* 20, 3578–3586. doi: 10.1029/2004gl021541
- Smith, E. M., and Kemp, W. M. (1995). Seasonal and regional variations in plankton community production and respiration for Chesapeake Bay. *Mar. Ecol. Prog. Ser.* 116, 217–231. doi: 10.3354/meps116217
- Sorte, C. J., and Bracken, M. E. (2015). Warming and elevated CO₂ interact to drive rapid shifts in marine community production. *PLoS ONE* 10:e0145191. doi: 10.1371/journal.pone.0145191
- Tait, L. W., and Schiel, D. R. (2013). Impacts of temperature on primary productivity and respiration in naturally structured macroalgal assemblages. *PLoS ONE* 8:e74413. doi: 10.1371/journal.pone.0074413
- Valiela, I. (1995). *Marine ecological processes, 2nd Edn.*, New York, NY: Springer-Verlag.
- Wild, C., Huettel, M., Klueter, A., Kremb, S. G., Rasheed, M. Y., and Jørgensen, B. B. (2004). Coral mucus functions as an energy carrier and particle trap in the reef ecosystem. *Nature* 428, 66–70. doi: 10.1038/nature02344
- Yap, H., Montebon, A., and Dizon, R. (1994). Energy flow and seasonality in a tropical coral reef flat. *Mar. Ecol. Prog. Ser.* 103, 35–35. doi: 10.3354/meps103035
- Yvon-Durocher, G., Jones, J. I., Trimmer, M., Woodward, G., and Montoya, J. M. (2010). Warming alters the metabolic balance of ecosystems. *Philo. Trans. R. Soc. Lond. B Biol. Sci.* 365, 2117–2126. doi: 10.1098/rstb.2010.0038
- Zeebe, R. E., and Wolf-Gladrow, D. A. (2001). *CO₂ in Seawater: Equilibrium, Kinetics, Isotopes*. Houston, TX: Gulf Professional Publishing.

Conflict of Interest Statement: The authors declare that the research was conducted in the absence of any commercial or financial relationships that could be construed as a potential conflict of interest.

Copyright © 2016 Trnovsky, Stoltenberg, Cyronak and Eyre. This is an open-access article distributed under the terms of the Creative Commons Attribution License (CC BY). The use, distribution or reproduction in other forums is permitted, provided the original author(s) or licensor are credited and that the original publication in this journal is cited, in accordance with accepted academic practice. No use, distribution or reproduction is permitted which does not comply with these terms.